TEMPERATURE AND CONVECTIVE HEAT TRANSFERT COEFFICIENT PROFILES DOWNSTREAM A MULTIPERFORATED PLATE- APPLICATION TO COMBUSTION CHAMBER COOLING

PETRE Brice, DORIGNAC Eva,VULLIERME J.J
Laboratoire d'Etudes Thermiques.
U.M.R. C.N.R.S 6608-ENSMA.

Keywords : *full coverage film cooling, rows number, blowing rate, temperatures probings, convection heat transfer coefficient.*

Abstract

In this study, we take an interest in the full coverage film cooling, which is utilised to protect the combustion chamber walls. It consists in injecting cooling air coming from compressors through drilled holes. Those are often placed in staggered configuration like our case. This experimental study is based on temperatures and convection heat transfer coefficient profiles obtained upstream one from nine rows of holes. Three thermal cases are imposed with three blowing rates and for a same mainstream Reynolds Number. Profiles are obtained by thermocouples probings. It appears that five rows are necessary to form a protecting cold layer.

Nomenclature

General parameters :

D :	Hole diameter (mm).
$M= \rho_j U_j / \rho_\infty U_\infty$:	Blowing rate.
T :	Temperature (K).
x_1/D :	Distance from wall leading edge.
x_2/D :	Distance from last opened row.
φ_{diss} :	Electrical density (W/m^2).
L_p/D :	Penetration height.
L/D :	Hole length.

Greek symbols:

α:	Injection angle.
δ/D :	Dynamic boundary layer thickness at the injection hole .
δ_{cl}/D:	Cold layer thickness.
ρ :	Density (kg/m^3).

subscripts:

hc:	Hot case.
cc:	Cold case.
ac:	Average case.
j :	Evaluated at injection conditions.
∞ :	Evaluated at free stream conditions.
w :	Evaluated at the wall.
0 :	Without hole.
mes :	Measured temperature.

1 Introduction

Since the appearance of aeronautic propeller and the will to increase their performances, constructors are confronted to the problem of combustion chamber walls cooling. They're exposed to important convective and radiative heat flux. Hot gases can attend temperatures in the order of 2000K. Actual materials can't support these temperature levels. So it's important to protect them. The general principle consist in injecting, through the combustion chamber wall , a part of the air coming from compressors placed upstream. The most

currently injection type is the full coverage discrete hole film cooling (*D = 6/10 mm*) [1].

This thermal protection is based on three processes : a cooling upstream holes, an internal cooling (the most important) and the formation of a cold layer downstream holes. This layer is due to the jets union emerging from holes. This is this way of protect, which interests us.

The increase of cooling effectiveness is based on the study of geometric and aerothermic factors. Geometric factors are the injection hole diameter D, the lateral spacing p/D between holes and longitudinal spacing s/D between rows, the injection angle (simple or composed), the hole exit geometry (expanded or not), the hole length L/D and the in-line or staggered configuration.

Aerothermic factors are the blowing rate M [2], the boundary layer thickness at the injection point δ/D, the turbulence level Tu, the mainstream Reynolds Number based on the diameter Re_D, the temperature ratio T_j / T_∞ and density ratio ρ_j / ρ_∞.

An expanded exit gives a best protection downstream rows of holes [3, 4, 5], because for a same coolant rate, the injection velocity at the exit is less than an classical exit. So jets penetrate less in the boundary layer and spread more laterally. However, the way of drilling this hole configuration is very difficult and costly. The injection angle plays on the jet penetration and varies from 17° [6] to 90°. Actually, several studies are leaded in combining a second injection angle [7, 8], whose influence is a best lateral spread of jets and so the reduction of hot spots locations. But, it appears a great interaction between two streams and so, a great jets mixing in the mainstream.

In fact, we find not much works which treat of the successive rows opening and consequences on the wall temperature variation upstream those rows [9]. So, this experimental study treats about this influence on the cold layer development in geometrics and aerodynamics simples cases. It's based on the exploitation of temperatures profiles obtained by thermocouples probings downstream 1 to 9 rows of 8 holes (D = 6mm). Three thermal cases are imposed and three blowing rate are studied. Holes are in staggered configuration and results are compared with the case without injection.

2 Experimental apparatus

Experiments have been made in a study canal, which was traversed by a mainstream and an injected stream. This canal is constituted by an injection wall and an opposite probing wall. The mainstream is generated by 2 blowers placed in parallel configuration. They're independently associated to flowmeter panels to control the total flowrate Q_∞ . This mainstream can be heated with an electrical resistance up to 80°C or cooled in passing in an heat exchanger up to 16°C. The electrical resistance or the heat exchanger is placed downstream the flowmeters panels. Calculations of Q_∞ are based on temperatures changes between the exit of the blowers (T_{exit} = 40°C) and the one in the canal T_∞.

The injected stream at room temperature T_j, is generated by a depressor placed downstream the canal. It aspires both the mainstream and the injected stream (fig.1, fig.2):

$$Q_d = Q_\infty + Q_j.$$

At the time of the first row opening, a total pressure probe has been placed perpendicularly to the internal wall hole and has allowed to calibrate (without mainstream) the desired injection rate. At late, it was possible to control the injection rate with a manual valve placed between the canal and the depressor.

The injection wall, firstly full, can be drilled from 1 to 9 rows of 8 holes placed in staggered configuration. The hole diameter is *D = 6mm* and its angle is $\alpha = 90°$. Lateral and longitudinal spacings are the same and fixed at *p/D = s/D = 6* (fig.3). The first row is situated at 5.5D from the injection wall leading edge . This one is constituted by three materials. The first, in contact with streams, is an epoxy plate equipped with 4 printed circuits allowing to generate an identical and known parietal density $\varphi_{diss}(W/m^2)$.(fig.4). The second is an altuglass plate and, at last the third is an isolate plate in

styrodur. So the injection wall gives a length to diameter *L/D = 6.9*.

The probing wall permits the intrusion of a comb fixed on an inflexible stem and equipped with 3 type K thermocouples ($D_{Thermocouple}=0.2mm$). The wall is equipped with 15 removable and airlight stoppers. Their placement is provided to measure three temperature profiles 3D downstream the row at three lateral locations: *y/D = -1.5, 0* and *1.5*. (fig.5). A special stopper, drilled and equipped with a toric joint, permits the stem perpendicular displacement with respect to the injection wall. Type K thermocouples have been mounted within the wall and along it in front of each stopper. They allow us to calculate, after thermal balance, the wall temperature $T_w(y/D=0)$ in contact with the fluid. A numeric simulation using Nodal Method has been done to verified the injection velocity influence on the conduction heat transfer through the wall. It appears that there's no influence at the thermocouple location (red star on Fig 9.)

An other placed at the canal entry permits to measure and control T_∞ ,and at first, one situated near the injection exit gives T_j.

3 Measurement techniques

Measurements are based on the establishment of 3 temperature profiles. The comb displacement is assumed by a step by step motor (type *Charlyrobot* with microprocessor (3.5 A – 44V, type 19936)). This motor fixed on a displacement rail, permits the probing stopper after stopper. Displacements and acquisition central *HP3497A* are piloted by a computer and a *HP-VEE 4.01* program. For each displacement and thermocouple, the sampling is 25 measurements with a frequency equal to 10Hz. An average value is recorded in an only file.

Three displacement zones with different steps have been imposed:

- a first zone near the wall with a D/3 thickness and an initial step of 0.1mm after contact and 10 steps of 0.2mm.
- a second intermediary zone with a 2D/3 thickness and 10 steps of 0.4mm.
- a third far away zone with variable thickness from 7D to 11D with steps of 1mm.

4 Results and discussion

4.1 Thermal cases presentation

Cases illustrated on (fig.6), present different experimental thermal conditions and their analysis. For 5 rows, and *M=2*, temperature profiles have been non-dimensioned et compared with the case without injection. Those conditions are:

1. cold case (cc): $T_\infty / T_j = 1$, $\varphi_{diss} = 500W/m^2$.
2. average case (ac): $T_\infty / T_j = 1.06$, $\varphi_{diss} = 350W/m^2$.
3. hot case (hc): $T_\infty / T_j = 1.15$, $\varphi_{diss} = 100W/m^2$.

The Reynolds number based on the hole diameter and the average mainstream velocity U_∞ in the canal is equal to $Re_D = 630$, so $\delta/D = 0.46$ at the injection location. The cold case allows the determination of an heat coefficient h_{cc} downstream holes and the comparison with the case without protection h_{cc0}. However, temperature profiles show the part of the cooling because $T_{cc(z/D=0)}^* = (T_{mes}-T_\infty) / (T_{wcc0} - T_\infty) = 0.5$ at $y/D = 0$. Average and hot cases are essentially different in the choice of the origin slope sign. Temperature profiles give a height of penetration L_p/D and a cold layer thickness δ_{cl}/D (fig.6b,6c) . For these cases, the jet centre is situated at $L_p/D = 2$ from the wall (minimum of $T_{ac}^* = (T_{mes} - T_j) / (T_\infty - T_j)$ and T_{hc}^*) and the cold layer thickness is estimated at $\delta_{cl}/D = 6$.

Following graphics present variations of h_{cc}, $T_{wac}^* = (T_{wac} - T_j) / (T_\infty - T_j)$ and $T_{whc}^* = (T_{whc} - T_j) / (T_\infty - T_j)$ along the wall. Indeed, h_{cc} variation admits a maximum downstream the 4th row at $x_1/D = 26.5$ and takes a value of $29W/m^2/K$. T_w^* variations for hot and average cases, confirm the important part of cooling in

the drilled zone. T_{wac}* = 1.2 compared to 2 (no rows) and T_{whc}* = 0.7 compared to 0.98 at x_1/D = 26.5. It confirms too the fast lost of protection downstream the last drilled row.

4.2 Blowing rate influence

The manual valve allows to impose different blowing rates. The canal thickness, being equal to 100mm for a hole diameter of 6mm, the blowing rate have been chosen to avoid impinging jets on the opposite wall. So, values are *M = 1, 2* and *5*. Three thermal cases have been imposed for each blowing rate. Graphics, presented (fig.7), show T_{hc}* variations 3 diameters downstream 5 rows of holes. For the case *M = 1*(fig.7a), the jet stays near the wall and give a value T_{whc}* = *0.73* at *y/d = 0*. It appears that height of penetration is *Lp/D = 0.6* with a cold layer thickness δ_{cl}/D= *4*. For the case *M=2* (fig.7b), T_{whc}* = *0.72* at *y/D = 0* , L_p/D = *2*, δ_{cl}/D= *6*. For *M = 5* (fig.7c), measurements give T_{whc}* = *0.7*, L_p/D = *4*, δ_{cl}/D= *11*.

The cold case gives variations of h_{cc}* = h_{cc} / h_{cc0} function of M along the wall. It appears that, for each blowing rate, the values are higher after the 4th row. A little decrease becomes after the 5th row for *M = 1* and *M = 2* and is most important for *M = 5*. It results from an higher jets penetration for this blowing rate and so a lower protection at *y/D = 0*. For *M = 1* and *M = 2*, jets penetrate less in the cold layer and homogenise themselves with this one. So h_{cc}* values after the 4th and the 5th row are sensibly equals and it shows the cold layer is formed after 5 rows. T_w* / T_{w0}* variations for hot and average cases along the wall allow to visualise directly the blowing rate influence in the drilled zone and downstream this one. Downstream the 5th row, the cooling is higher for the greatest M. However, for x_1/D = *44.5* and *M = 5*, emerging jets from the 5th row seem to reattach to the wall. h_{cc}* variation confirm this hypothesis, because it appears a level at this point.

But, in the drilled zone, the blowing rate influence seems to be more complex. For the hot case and *M = 1*, T_{whc}* / T_{whc0}* values are below than those obtained with others blowing rate from 2 rows to 5 rows. The fact, that for a small M, jets stay near the wall, explain certainly this phenomenon. But the low injected rate doesn't allow to maintain an important cooling downstream five rows. For all cases, downstream the last drilling row, T_w* / T_{w0}* variations are conditioned by the blowing rate and follow a similar behaviour. They show the cold layer homogeneousness, whose thickness is directly function of the blowing rate M.

4.3 Rows number influence

The complete study allows to trace h_{cc}* and T_w* / T_{w0}* variations for several opened rows and for the three blowing rate (fig.8). h_{cc}* variations confirm that the cold layer is formed after 5 rows. Beyond x_1/D = *32.5* and for *M = 1, 2* and *5*, it appears a level, which is maintained for a row number greater than five. However, beyond the last opened row, the fast decrease of h_{cc}* shows the cold layer effectiveness is rapidly reduced if it isn't maintained.

In every cases, three T_w* / T_{w0}* variation zones at the location *y/D = 0* could be schematised :

- the drilled zone (from the 1st row to the next to last), where T_w* / T_{w0}* decreases regularly and identically as and when rows are opened.
- the 6D length zone downstream the next to last row, where T_w* / T_{w0}* increases symmetrical about the decrease.
- the last zone where T_w* / T_{w0}* increases regularly to unity.

This scheme is verified for the h_{cc}* variation. In fact, it appears it exits a maximum for each variation. This maximum placement (x_m/D) squares with the T_w* / T_{w0}* minimum placement for the same opened rows number. Is there a relation between h_{cc}* calculated when T_∞ / T_j = *1* and T_w* / T_{w0}* ($T_\infty / T_j \neq 1$). Considering that thermal cases have the same Reynolds number and the same Prandt number, they're similar. So the Nusselt number variation $Nu = h_{cc}*D/\lambda_{cc}$ could be the same along the wall. A reference temperature T_{ref} has been

evaluated in considering h_{cc} which was evaluated with the cold case:

$$T_{refhc} = (\varphi_{cv} * \lambda_{cc}) / (h_{cc} * \lambda_{hc}) - T_{whc}$$

$$T_{refac} = (\varphi_{cv} * \lambda_{cc}) / (h_{cc} * \lambda_{cm}) - T_{wac}$$

Results aren't decisive but, an other way to compare the three thermal cases is looked for.

5. Conclusion

The objective of this study was to understand the rows number influence on the full coverage film cooling, which intervenes in the wall combustion chamber protection. For a simple geometry (from 1 to 9 staggered rows of 8 holes, *D=6mm, α = 90°, p/D = s/D = 6*) and for 3 thermal cases, we have observed the blowing rate influence M (*M=1, 2* and *5*) on $h_{cc}^* = h_{cc} / h_{cc0}$, T_{wac}^* / T_{wac0}^* and T_{whc}^* / T_{whc0}^* variations at the *y/D = 0* location.

Temperature profiles, obtained with type K thermocouples in drilled zone and downstream this one, show that five rows are necessary at the film cooling formation. Moreover this cold layer completely formed for 9 rows, collapses rapidly if it isn't maintained. It exists surely a relation between h_{cc}^* and T_w^* / T_{w0}^* variations. Those variations can be schemed by three zones: the drilled zone to the next to last row, a symmetrical 6D length zone and at last the return to the zero protection.

6. References

[1] J.L Champion, « Etude expérimentale des films pariétaux de refroidissement produits par une paroi multiperforée. Cas des conditions de fonctionnement des chambres de combustion de moteurs aéronautiques », 1997, Thèse de l'Université de Poitiers.

[2] S. Yavuzkurt, R.J. Moffat, W.M. Kays, « Full-coverage film cooling. Part 1. Three-dimensional measurements of turbulence structure », « Full-coverage film cooling. Part 2. Prediction of the recovery-region hydrodynamics », 1980, *J. Fluid. Mech*, Vol 101, pp129-178.

[3] R.J. Goldstein, E.R.G. Eckert, F. Burggraft, « Effect of hole geometry and density on three-dimensional film cooling », 1973, *Int.J.Heat Mass Transfer*, Vol. 17, pp 575-607.

[4] E.Dorignac, B. Petre, J.J Vullierme, « Etude comparative du refroidissement par film en aval d'une rangée de jets a section de sortie soit cylindrique soit évasée », presented at the SFT 1998, Marseille.

[5] K. Thole, M. Gritsch, A. Schulz, S. Wittig, « Flowfield measurements for film cooling holes with expanded exits », 1998, ASME Journal of Turbomachinery, Vol 120, pp327-335.

[6] M. Martiny, A. Schulz, S. Wittig, « Full Coverage Film Cooling Investigations: Adiabatic Wall Temperatures and Flow Visualisation », 1995, *ASME Paper 95-WA/HT-4*. Presented at the International Mechanical Engineering Congress & Exposition San Francisco, California- November 12-17, 1995.

[7] P.M. Ligrani, J.M. Wigle, S. Ciriello, S.M. Jackson, « Film cooling from holes with compound angle orientations: Part1- Results downstream of two staggered rows of holes with 6d spanwise spacing », 1994, *Transaction of the ASME Journal of Heat Transfer* , May, Vol. 116, pp353-362.

[8] S. Honami, T. Shizawa, A. Uchiyama, « Behaviour of the laterally injected jet in film cooling: measurements of surface temperature and velocity/temperature field within the jet », 1994, *Transaction of the ASME Journal of Turbomachinery*, January, Vol.116, pp106-116.

[9] B. Petre, E.Dorignac, J.J Vullierme, « Etude aérodynamique de l'interaction de multirangées de jets placés en quinconce avec un écoulement transversal : application au refroidissement par multiperforation. », presented at the 35ème colloque d'aérodynamique appliquée AAAF, Lille- Mars 22-24,1999.

Experimental apparatus

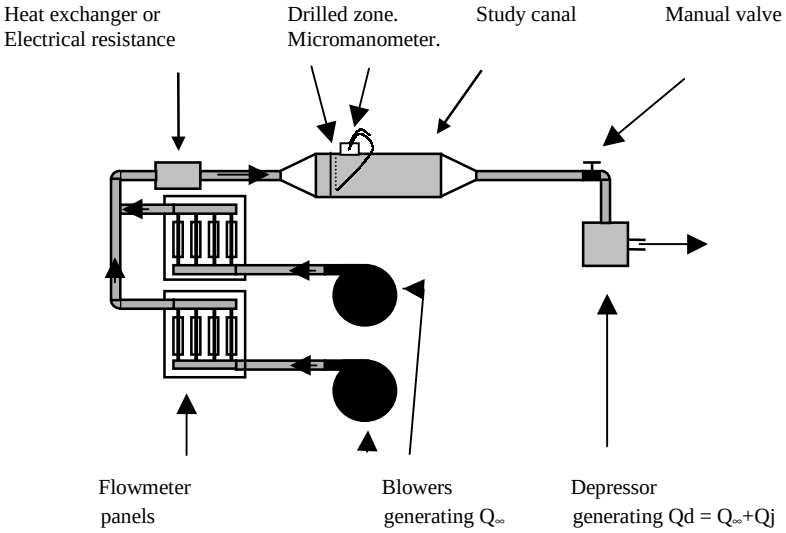

Fig.1 General view.

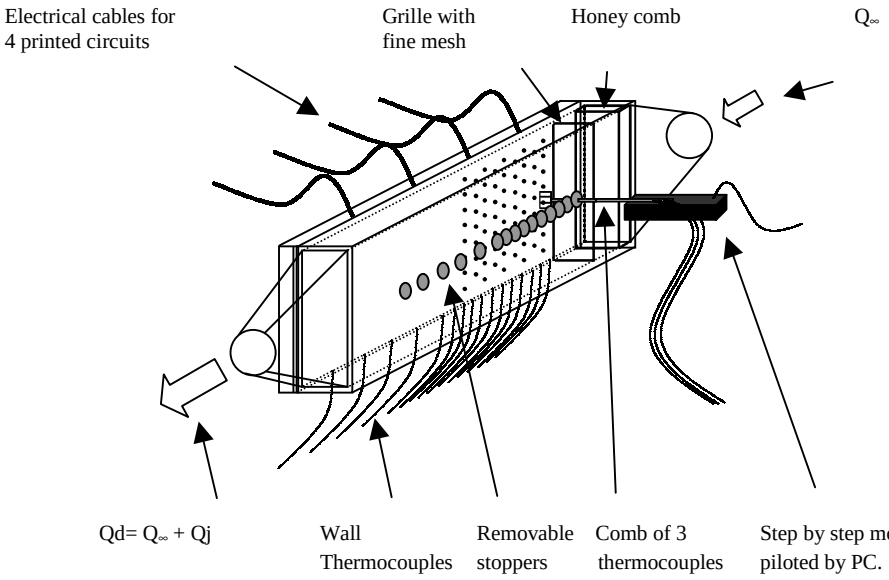

Fig.2 Canal view.

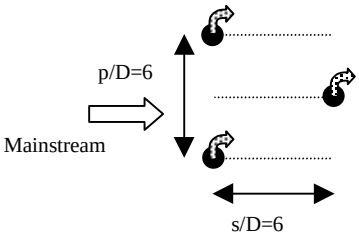

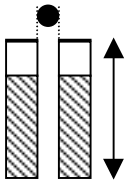

Epoxy with circuit.
Altuglass
L/D=6.9
Styrodur

Fig3. Holes configuration.

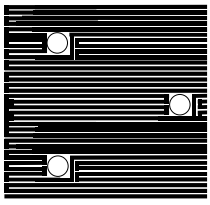

Fig4. Printed circuit.

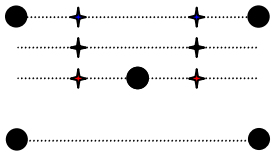

y/D = 1.5
y/D = 0
y/D = -1.5

Fig5. Probing locations.

Fig.6. Thermal cases presentation.

5 Rows, M=2. Non-dimensioned temperature profiles. $x_1/D = 32.5$, $x_2/D = 3$. $Re_D = 630$.

Variation of h_{cc}, T_{wac}* and T_{whc}* along the wall. Comparison with no rows cases.

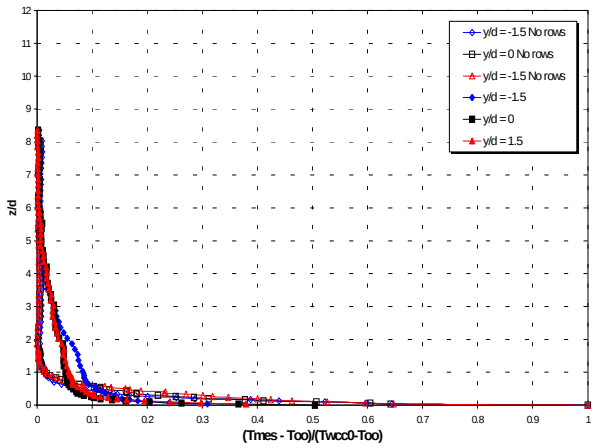

a. Cold case. $T_\infty / Tj = 1$, $\varphi_{diss} = 500$ W/m^2.

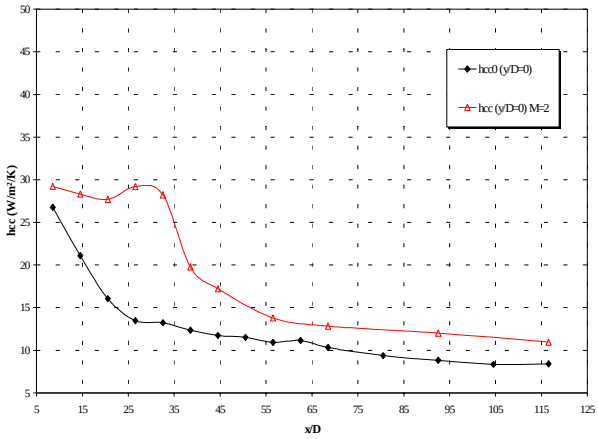

Cold case. h_{cc}*

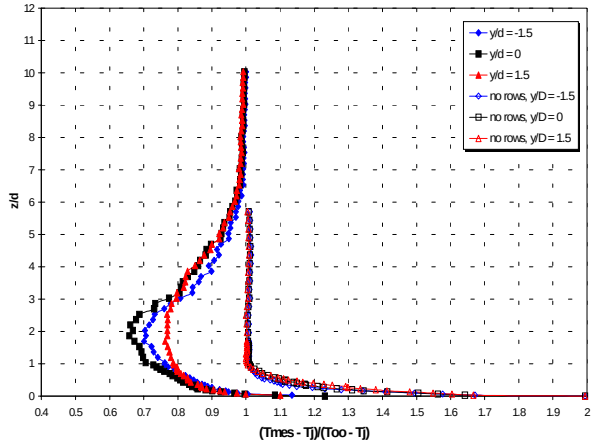

b. Average case. $T_\infty / Tj = 1.06$, $\varphi_{diss} = 350$ W/m^2.

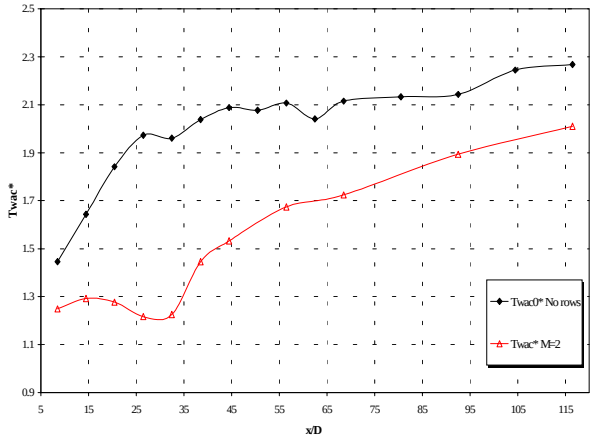

Average case. T_{wac}*.

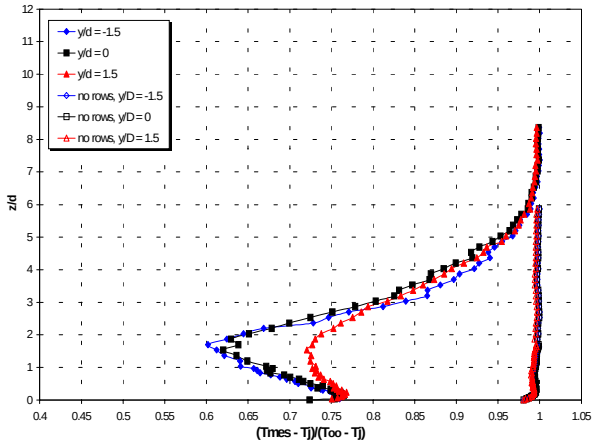

c. Hot case. $T_\infty / Tj = 1.15$, $\varphi_{diss} = 100$ W/m^2.

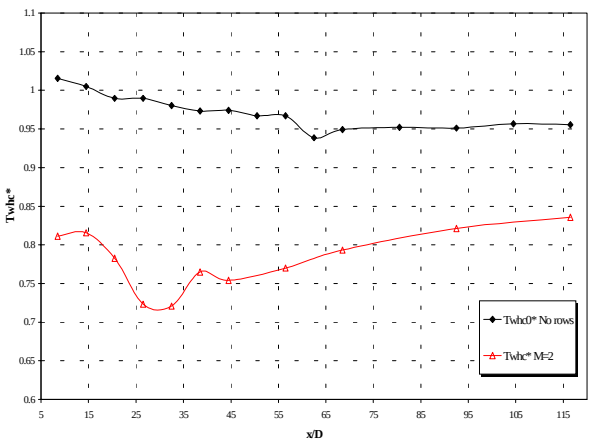

Hot case. T_{whc}*.

Fig.7. Blowing rate influence

5 rows. M = 1, 2 and 5. x_1/D = 32.5, x_2/D = 3. Re_D = 630.

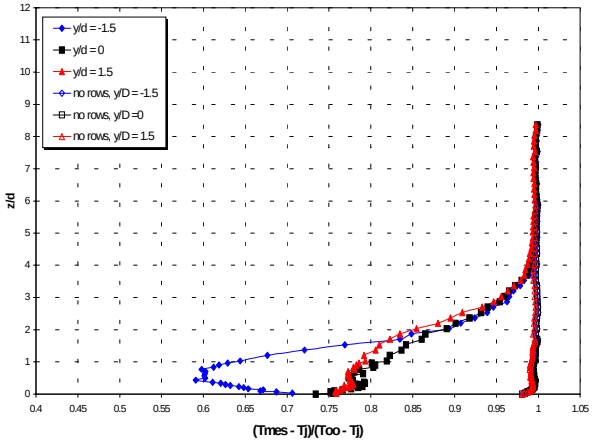

fig7.a. hot case. M=1.

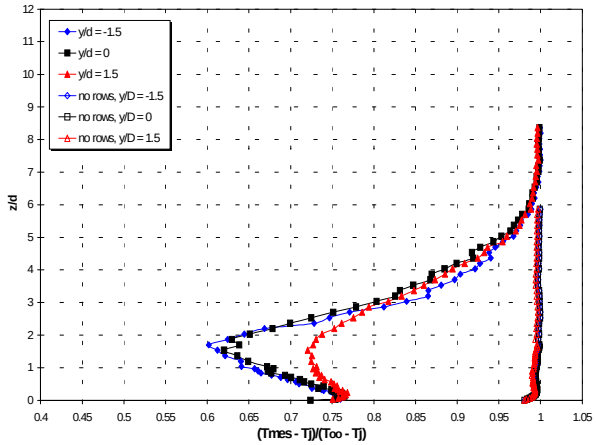

fig7.b. hot case. M=2.

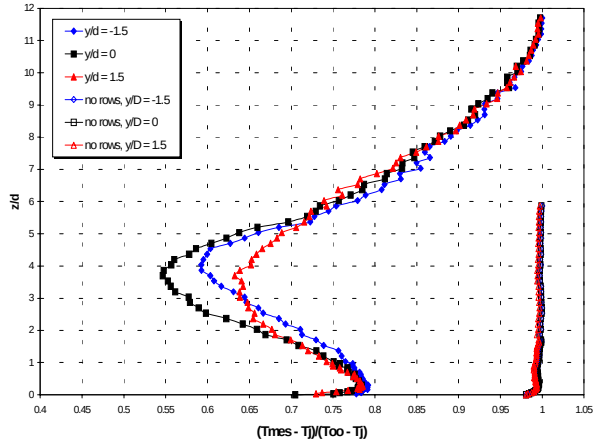

fig7.c. hot case. M=5.

Evolution of $h_{cc}^* = h_{cc} / h_{cc0}$, T_{wac}^*/ T_{wac0}^* and T_{whc}^*/ T_{whc0}^* for M = 1, 2 and 5.

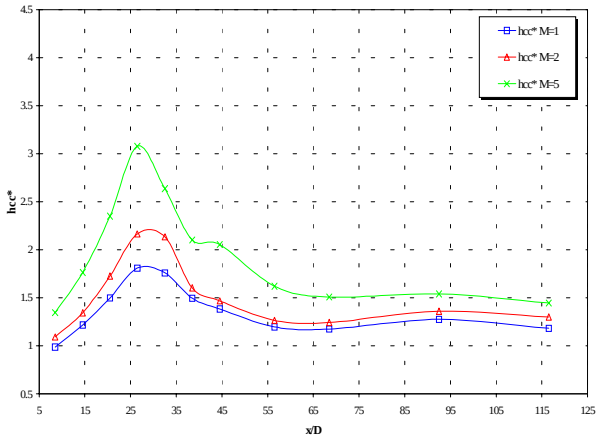

Cold case. h_{cc}^* along the wall.

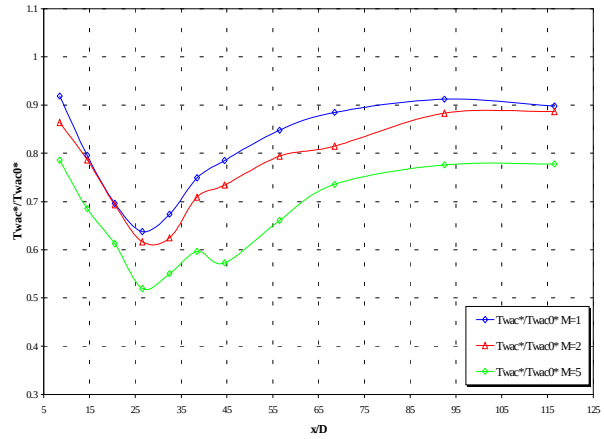

Average case. T_{wac}^*/ T_{wac0}^*along the wall.

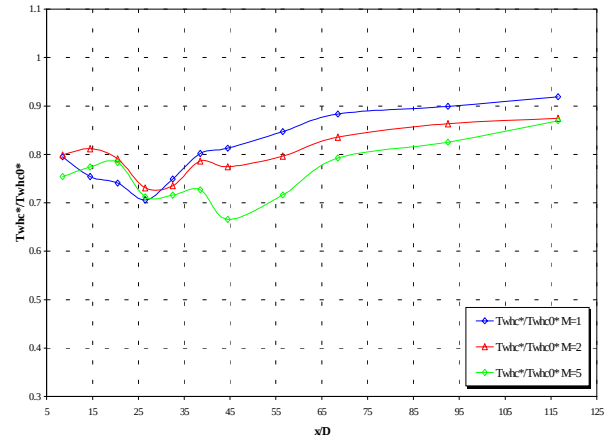

Hot case. T_{whc}^*/ T_{whc0}^*along the wall.

Fig.8. Rows number influence

For M = 1, 2 and 5. From 0 to 9 rows.

Evolution of h_{cc}*. **Cold case**.

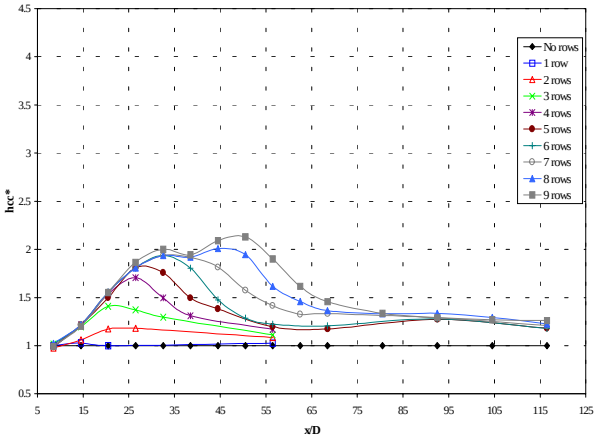

M=1.

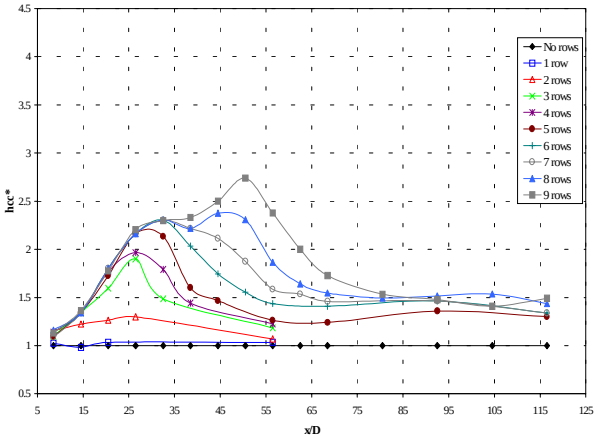

M=2.

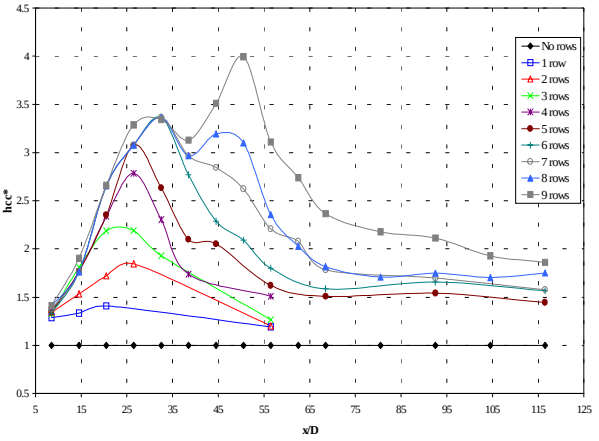

M=5.

Evolution of T_{wac}*/ T_{wac0}* along the wall.

From 0 to 9 rows. **Average case**.

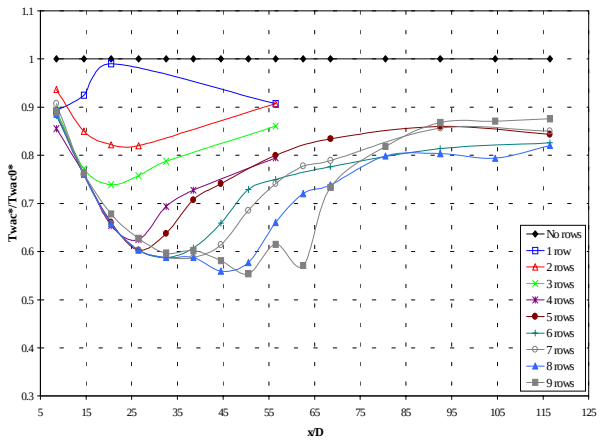

M=1.

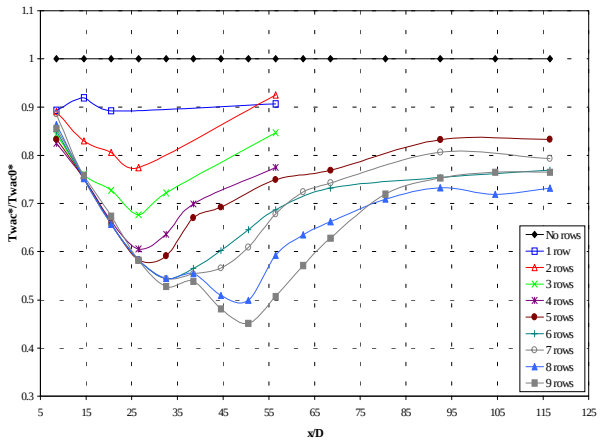

M=2.

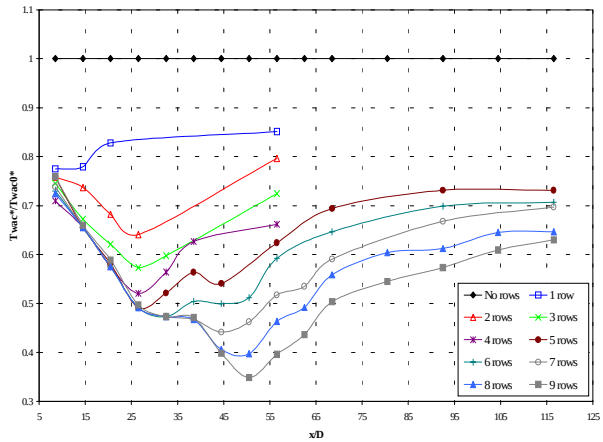

M=5.

Evolution of T_{whc}*/ T_{whc0}* along the wall.

From 0 to 9 rows. **Hot case**.

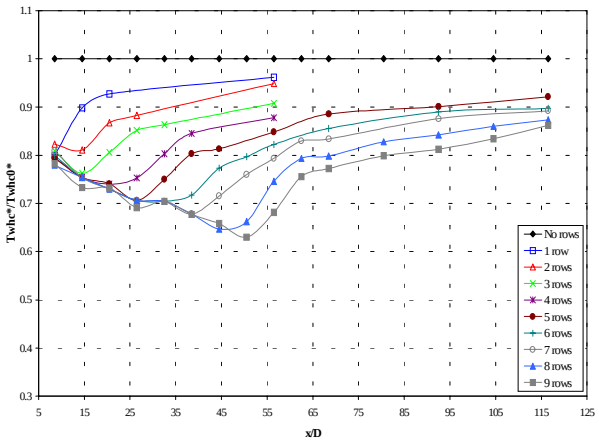

M=1.

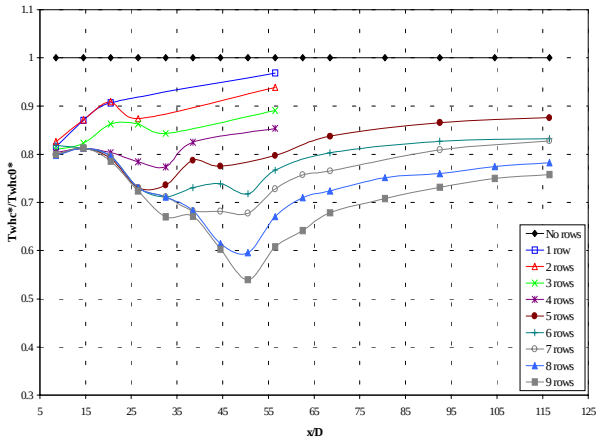

M=2.

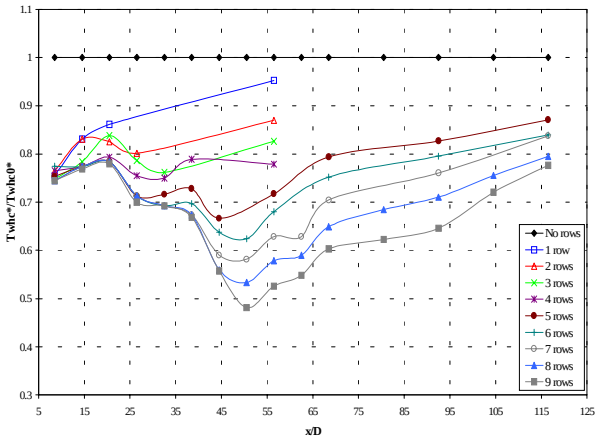

M=5.

Fig 9. Numeric simulation. Hot case, $h_{upstream}$ and $h_{downstream}$ fixed, h_{hole} calculated with Colburn correlation for M=1, 2 and 5.